Plasma Electron Trapping and Acceleration in a Plasma Wake Field Using a Density Transition

H. Suk, N. Barov, and J. B. Rosenzweig
Department of Physics and Astronomy
University of California Los Angeles
Los Angeles, CA 90095

E. Esarey
Center for Beam Physics,
Ernest Orlando Lawrence Berkeley National Laboratory,
Berkeley, CA 94720

Abstract

A new scheme for plasma electron injection into an acceleration phase of a plasma wake-field is presented. In this scheme, a single, short electron pulse travels through an underdense plasma with a sharp, localized, downward density transition. Near this transition, a number of background plasma electrons are trapped in the plasma wake field, due to the rapid wavelength increase of the induced wake wave in this region. The viability of this scheme is verified using two-dimensional particle-in-cell (PIC) simulations. To investigate the trapping and acceleration mechanisms further, a 1-D Hamiltonian analysis, as well as 1-D simulations have been performed, with the results presented and compared.

PACS Codes: 52.40.Mj, 52.75.Di, 29.17.+w, 29.27.-a

Accepted for publication in *Physical Review Letters*

Compared to standard radio-frequency linear accelerators, advanced accelerators using plasmas can produce much higher acceleration gradients, in excess of 1 GeV/m. Hence, extensive research on plasma-based accelerators [1-4] has been performed in recent years. For plasma-based accelerators, short, intense laser (laser wake field accelerator, or LWFA) or electron beam (plasma wake field accelerator, or PWFA) pulses are used to drive large amplitude plasma waves. In these schemes, the maximum achievable accelerating gradient scales as the nonrelativistic plasma frequency, $\omega_p = (4\pi n_0 e^2 / m_e)^{1/2}$. Here n_0, e, and m_e denote the plasma density, electron charge, and electron mass, respectively. Thus high gradient operation implies use of short period waves, and in order to obtain a beam with small energy spread, an ultra-short (<< 1 ps) accelerating pulse must be injected into such a system. This requirement, however, is difficult to meet with an external injector, especially in the case of the LWFA. The challenge of injection in the LWFA has led to proposals of all-optical plasma electron injection schemes using two [5] or three laser pulses [6]. However, these optical methods require extremely accurate laser spatial and temporal overlap, which again leads to technical difficulties.

To avoid these problems, Bulanov *et al.* [7] proposed a self-injection scheme using a single laser pulse propagating in an inhomogeneous plasma. In their scheme, trapping of background plasma electrons occurs from wavebreaking induced by a gentle density decline, in which the density scale length $L_s = n_0 / |dn_0 / dz|$ is much larger than the plasma skin depth $k_p^{-1} = v_b / \omega_p$, where $v_b \quad c$ is the driving pulse's group velocity. As the laser pulse propagates down the density gradient, the phase velocity of the wake gradually decreases until it becomes equal to the plasma fluid oscillation velocity, which results in conventional wavebreaking. Bulanov's scheme is much simpler than other plasma injection methods, but leads to an injected beam pulse with a relatively large phase spread. In addition, the accelerating and focusing fields in a typical LWFA are relatively nonuniform and may not give as high of beam quality as the blowout regime of the PWFA [8,9], in which a plasma electron-rarefied region is formed in the wake of the driving electron beam. Inside of this rarefied region, an accelerating electron experiences acceleration dependent only on longitudinal position, and focusing which is linear in offset from the axis, just as in more conventional accelerators. Furthermore, beam electrons in this PWFA scheme experience less scatter with background plasma electrons during acceleration. Thus superior beam quality is expected from the PWFA in this regime.

In this Letter, we propose a new self-injection scenario for the PWFA in the blowout regime, where the beam density greater than the plasma density, $n_b > n_0$ (underdense condition). It is known that in the one-dimensional (1-D) limit of a PWFA with uniform

plasma density, self-trapping of background electrons by the wave is very difficult [10,11]. Further, it is observed in two-dimensional (2-D) simulations of the PWFA in the blowout regime that self-trapping in a uniform plasma is even more difficult when transverse motion is allowed. To achieve self-trapping in the PWFA, we propose to introduce a sharp, localized density gradient. In this scheme, a single short electron beam pulse is sent through an underdense plasma with a sharp downward density transition with $k_p L_s < 1$, marking the boundary between a dense upstream region (*I*) and a less dense downstream region (*II*). When the beam passes a sharp downward plasma density transition, the wavelength of the plasma wave changes rapidly. In this situation, the plasma electrons that originate just inside region *II* spend much of their oscillation in region *I* before returning to near their initial position in *z*, advanced in wave phase compared to the nominal (uniform plasma) region *II* oscillation. At this position, normally (for a uniform plasma) the electron is phased in the wake such that the electric field is zero, but in the case we now consider, the faster oscillation of the electron in region *I* allows the electron entering region *II* to remain in an accelerating phase. This proposed dephasing mechanism, which is justified in qualitative and quantitative detail below, allows plasma electrons to be trapped and accelerated in region *II*. This phenomenon is shown in Fig. 1, which displays a 2-D particle-in-cell (PIC) simulation using the code MAGIC. This injection mechanism is fundamentally different from Bulanov's gentle density gradient scheme for the LWFA. In Bulanov's case, plasma electrons are trapped in the second plasma oscillation period, but they arise from wavebreaking in the first period. On the other hand, in the present scheme, plasma electron trapping occurs in the first rarefied cavity, due to localized nonlaminar motion near the sharp density transition, and at wake amplitudes well below conventional wavebreaking.

We have explored density transition-induced particle trapping using 2-D PIC simulations (both MAGIC, and a UCLA-specific code NOVO-PIC) in order to illuminate the physical mechanisms relevant to the trapping process. The MAGIC results shown in Fig. 1 were obtained with an ambient plasma density of $n_0^I = 5 \times 10^{13}$ cm^{-3} for $k_p^{II} z < 11.2$, and $n_0^{II} = 3.5 \times 10^{13}$ cm^{-3} for $k_p^{II} z \geq 11.2$, plasma electron temperature $kT_e = 3$ eV, and stationary ions. Here we parameterize lengths in terms of the plasma skin depth in region *II*, $k_p^{II} = \sqrt{4\pi n_0^{II} e^2 / m_e c^2}$. The ultra-relativistic (16 MeV) drive beam density distribution employed in the simulation was chosen as a bi-Gaussian $n_b(r,\xi) \sim e^{-r^2/2\sigma_r^2} e^{-\xi^2/2\sigma_z^2}$ ($\xi = z - v_b t$), with peak density $n_b = 5 n_0^I = 3 n_0^{II}$, and dimensions $k_p^{II}\sigma_z = 1$, $k_p^{II}\sigma_r = 0.28$. In Fig. 1(a) we observe the trapped population of electrons just as they

return to near their initial position (beam at $k_p{}^{II}z = 18.6$), and the associated structure of the wake, which is somewhat complicated at this point. Two features are clearly shown, however: a clear difference in wave frequencies between regions *I* and *II*, and a local breaking of the wave near the boundary. In Fig. 1(b), it is seen that, after traversing an additional few plasma wavelengths past the boundary (beam at $k_p{}^{II}z = 35.2$), the trapped plasma electron bunch is loaded into a well-behaved blow-out regime wave. Furthermore, this injected electron population is transversely controlled by uniform ion-focusing in the blow-out region.

The longitudinal phase space of the plasma electrons at the two times corresponding to Figs. 1(a) and 1(b) are shown in Fig. 2. Figure 2(a) shows a significant amount of plasma electrons are injected into the accelerating wave. Figure 2(b) shows that the trapped plasma electron population (in the range of 5 ~ 15 MeV/c) have attained excellent separation in momentum from the background plasma. The population of trapped particles occupies a longitudinal phase extent of $9\phi \setminus 5\pi$ 9%, with a large charge of about 0.5 nC for these parameters. Careful comparison of Figs. 2(a) and 2(b) indicates very little phase slippage of the trapped electrons during acceleration. With such a small beam phase extent, it would be possible to simply compensate the momentum spread by slowly lowering the plasma density further, to rephase the trapped electrons to forward in the wave.

In systematic simulation studies of this scheme, we varied the characteristics of the density transition: the sign of density change, the amplitude of the density difference across the transition, and the density transition scale length. In all simulations, the driving beam and plasma characteristics were kept similar, in which blowout is complete and the plasma electron motion is both nonlinear and moderately relativistic. In these studies we observed trapping only in the case of a downward (in the direction of the beam travel) density transition. In addition, it was found that the number of trapped particles increased as the amplitude of density decrease was made larger. Finally, if the length over which the density was linearly decreased from its initial to final value becomes larger than a plasma skin depth $k_p{}^{-1} = c/\omega_p$, then the trapping disappears completely.

A further, definitive clue as to the trapping mechanism is that the trapped electrons all initially dwell, as stated above, in region *II*. These observations have led to the development of our trapping model, in which the initial motion of the plasma electrons is in the negative *z* direction (as well as the positive radial direction) under the forces induced by the drive beam. Upon entry into region *I*, the electrons experience wave fields which have a shorter oscillation wavelength, and can be dephased and trapped. This model also

qualitatively explains why we must have $k_p L_s < 1$. If it is the scale length is longer than the oscillation distance in *z*, then the plasma electrons cannot access the region of significantly higher plasma electron density.

At this point, we would like to place our model on firmer analytical ground. As a useful 2-D analytical model of plasma electron motion in the blowout regime does not exist, we proceed to develop a 1-D, fully relativistic analysis of plasma motion in both regions, and propose a scenario in which the motion of the plasma electrons is not strongly affected by the existence of the transition. A Hamiltonian analysis of the phase space trajectories of trapped electrons is thus made possible. This analytical model is then compared to the results of 1-D PIC simulations, in order to verify aspects of the model, and also point to its limitations. Without discussing any model details, some limitations are immediately apparent. First, in the blowout regime, the plasma electron density tends to vanish in the wake of the drive beam, while in 1-D nonlinear wave theory, the plasma density does not drop below one-half of the initial density n_0. In addition, a 1-D wave driven by an electron beam is somewhat of a practical improbability, as it implies total beam charge in excess of what is presently found. Nonlinear 1-D plasma waves may be driven by ultra-short laser pulses, however, and so the present analysis may have some direct application to density transitions in the LWFA. Note that a large amplitude, nonlinear wave is necessary to allow the trapping process we wish to describe, since for waves with amplitudes well below the wavebreaking limit, the plasma electrons do not move appreciably from their initial position, and do not attain relativistic oscillation velocities.

We begin the analysis by reviewing nonlinear 1-D plasma wake field theory, which has its basis in the fundamental work of Akhiezer and Polovin [12-15]. In this theory, with the wave *ansatz* assumed (all system spatial and temporal dependences can be expressed using $\tau = \omega_p (t - z/v_b)$), the differential equation governing relativistic cold fluid takes the following form,

$$\frac{d^2}{d\tau^2}\left[\frac{1-\beta_b\beta}{\sqrt{1-\beta^2}}\right] = \beta_b^2\left[\frac{\beta}{\beta_b-\beta} + \frac{n_b}{n_0}\right], \qquad (1)$$

where n_b is the beam density, $\beta_b = v_b/c$ is the normalized beam (as well as wave phase) velocity, and $\beta = v/c$ is the normalized plasma electron velocity.

Since the plasma wave is impulsively excited by the driving beam, we concentrate on the plasma dynamics in the region behind the beam. There, for a very relativistic beam

($\beta_b \rightarrow 1$), Eq. (1) can be rewritten as

$$x'' = \frac{1}{2}\left[\frac{1}{x^2} - 1\right] \quad \text{with } x = \sqrt{\frac{1-\beta}{1+\beta}}, \tag{2}$$

where the prime denotes $d/d\tau$. Equation (2) is equivalent both to the Poisson equation and the plasma electron equation of motion, so we can write the field and plasma fluid quantities, i.e., density, $\frac{n}{n_0} = \frac{1}{2}\left(1 + \frac{1}{x^2}\right)$, potential, $-e\phi = m_e c^2 (1 - x)$, and electric field, $-eE = k_p m_e c^2 x'$; as well as the dynamical quantities $\gamma = \frac{1}{2}\left(x + \frac{1}{x}\right)$, $\beta = \frac{1-x^2}{1+x^2}$, and $\beta\gamma = \frac{1}{2}\left(\frac{1}{x} - x\right)$, only using x.

With these results, we can perform a Hamiltonian analysis of the plasma electron motion. In the Galillean frame moving with the wave, the Hamiltonian H is constant,

$$H = -e\phi + \gamma m_e c^2 - \beta\gamma m_e c^2 = m_e c^2 \left(1 - x_f\right) + m_e c^2 x_e . \tag{3}$$

Here the quantity x_f corresponds to the field (and the plasma fluid) properties, as outlined above, while $x_e \equiv \sqrt{(1-\beta_e)/(1+\beta_e)}$ describes the dynamical state of any electron, fluid or otherwise, injected into the system. As H is invariant, the difference $\Delta x = x_f - x_e$ is also constant. Knowledge of the value of H and the function x_f thus allows one to map the electron trajectories in phase space, and easily determine which trajectories are trapped. With H as written above, electrons with $\Delta x > x_{f,\min}$ are trapped, defined such that as $x_f \rightarrow x_{f,\min}$, x_e approaches zero and $\beta_e \rightarrow 1$. With this model in mind, we can now discuss the approximate effects of the density discontinuity.

In this analysis we assume that the density discontinuity can be approximately modeled by using the Hamiltonian analysis in both regions on either side of a sharp density transition. The fields on both sides of the moving (in the τ frame) density boundary are assumed to be correctly given by the wave analysis. Note that at the boundary, the value of x_f is discontinuous, which implies that H changes suddenly when the electron crosses the boundary. This discontinuity in H mathematically allows the trapping of initially cold plasma electrons (x_e 0) in an ultra-relativistic phase velocity wave.

We also note that, because the system is 1-D, at the density transition boundary (which moves backward in the wave frame at $-v_b \quad -c$) there is a self-consistent discontinuity in the electric field of $\Delta E = 4\pi\sigma$. Here σ is the net surface charge density "absorbed" by the boundary due to displaced electrons from the upstream side, and "emitted" by those that would be displaced to the downstream side. The field near the boundary is illustrated in Fig. 3, which displays $E(z)$ found by theory and simulation. While the peak field in the two regions is the same, the field in the downstream, high-density region changes more quickly, since the plasma frequency is higher.

Even though the electric field discontinuity at the density transition is self-consistent in terms of displaced charge, it is of course unphysical in the sense that the fluid electrons are not emitted or absorbed by the boundary between the two regions. The fictional absorption at the boundary is also conceptually at odds with the physical model of trapping, in which the plasma particles move significantly past the boundary. Nevertheless, we find some agreement with this model and 1-D PIC simulations, as shown in Fig. 3. Here we also display the simulation-derived electric field associated with the same physical parameters (beam surface charge density of 0.36 μC/cm^2, $n_0 = 3.5\times10^{13}$ cm^{-3} for z>0.5 cm, and $n_0 = 5\times10^{13}$ cm^{-3} for z<0.5 cm) as used in the analytical model. The agreement is quite good for the fields calculated in the region z<0.5 cm, which is the important zone for electron trapping dynamics, as we shall see.

In order to determine how to connect the distinct values of H in the two regions of interest, the position of the electrons as a function of τ must be known, from which we find the time of boundary crossing. This can be accomplished by integrating the velocity,

$$z = c\int_{t_1}^{t_2}\beta\,dt = \frac{c}{\omega_p}\int_{\tau_1}^{\tau_2}\left(\frac{\beta}{\beta-1}\right)d\tau = \frac{1}{k_p}\int_{\tau_1}^{\tau_2}\left(\frac{1-x_e^2}{2x_e^2}\right)d\tau\,. \tag{4}$$

In the special case of the fluid electrons, $x_f = x_e$, we have $k_p z = \frac{1}{2}\int\left[n(\tau)-n_0\right]d\tau$, a result which emphasizes that the wave fluid motion is initially in the negative direction, and arrives back at the starting position after one period.

Using the formalism we have developed, we can compare the dynamics of a trapped electron from the 1-D PIC simulation to that derived from the analytical model. The electron we follow in the simulation is initially located at $z = 5.1$ cm (1 mm downstream of the density transition). To employ the theoretical model, we must follow the electron initially in the low-density (downstream) region, calculate its position and momentum crossing the

transition using Eqs. (3) and (4), and connect the values of H across the boundary. This calculation is then repeated in the high-density (upstream) region, the final value of H in the downstream region is calculated, and the motion examined for trapping. The results of this exercise are shown in Fig. 4, which displays the phase space trajectory of the electron in both the model and simulation. Good agreement on the predicted trajectory is obtained in the region of negative momentum, as expected from the agreement of the fields in the upstream region (Fig. 3), while notable disagreement occurs when the electron re-approaches the density transition from the upstream side. This disagreement arises from the inconsistency of the discontinuous field model we have developed, because of non-negligible charges passing through (not stopping at) the transition. Note that even though the exact phase space trajectory in the transition region is not accurately predicted, the final phase of the electron after trapping is well predicted by the analytical model.

The PWFA-based self-injection scheme we have proposed in this paper demands further theoretical and numerical investigations of detailed issues such as beam quality of the trapped plasma electrons, dephasing, drive beam quality degradation in the plasma, etc., and this will be done in the near future. To verify this new injection scheme, we are planning an experiment with an existing argon plasma source [16], which was originally developed for the underdense plasma lens experiment at the Neptune Advanced Accelerator Laboratory of UCLA.

This work was supported by the U.S. Department of Energy, under contracts DE-FG03-92ER4069 3 and DE-AC-03-76SF0098.

References

[1] C.E. Clayton, et al., Phys. Rev. Lett. **70**, 37 (1993).

[2] K. Nakajima, et al., Phys. Rev. Lett. **74**, 37 (1995).

[3] C. W. Siders, Phys. Rev. Lett. **76**, 3570 (1996).

[4] F. Amiranoff, et al., Phys. Rev. Lett. **81**, 995 (1999).

[5] D. Umstadter, J. Kim, and E. Dodd, Phys. Rev. Lett. **76**, 2073 (1996).

[6] E. Esarey, et al., Phys. Rev. Lett. **79**, 2682 (1997); E. Esarey et al., Phys. Plasmas **6**, 2262 (1999).

[7] S. Bulanov, et al., Phys. Rev. E **58**, R5257 (1998).

[8] J.B. Rosenzweig, et al., Phys. Rev. A **44**, R6189 (1991).

[9] N. Barov, et al., Phys. Rev. Lett. **80**, 81 (1998); N. Barov, et al., Phys. Rev. ST Accel. Beams **3**, 011301 (2000).

[10] T. Katsouleas and W. B. Mori, Phys. Rev. Lett. **61**, 90 (1988).

[11] J.B. Rosenzweig, *Phys.Rev. A* **38**, 3634 (1988).

[12] A. I. Akhiezer and R. V. Polovin, Sov. Phys. JETP **3**, 696 (1956).

[13] R. D. Ruth and A. W. Chao, in *Laser Acceleration.* AIP Conf. Proc. **91**, Ed. P. Channell (AIP, New York, 1982).

[14] J.B. Rosenzweig, *Phys. Rev. Lett.* **58**, 555 (1987).

[15] C. B. Schroeder, et al., *Phys. Rev. E* **59**, 6037 (1999).

[16] H. Suk, et al., IEEE Trans. Plasma Sci. **28**, 271 (2000).

Figure Captions

Figure 1. Configuration space (r,z) distributions of the plasma electrons from the MAGIC code 2-D PIC simulation.

Figure 2. Longitudinal momentum versus z of the plasma electrons for Fig. 1(a) and (b).

Figure 3. Plot of the wake electric field in the two regions ($n_0 = 3.5 \times 10^{13}$ cm^{-3} for z>0.5 cm, and $n_0 = 5 \times 10^{13}$ cm^{-3} for z<0.5 cm). Solid line indicates the field in the region calculated from the analytical model, while the dashed line indicates the model-derived field in the conjugate region. The thick dotted line is the field calculated from a 1-D PIC simulation.

Figure 4. Phase space trajectory of a trapped electron originating 0.01 cm downstream of the plasma density transition, for the simulation and parameters of Fig. 1.

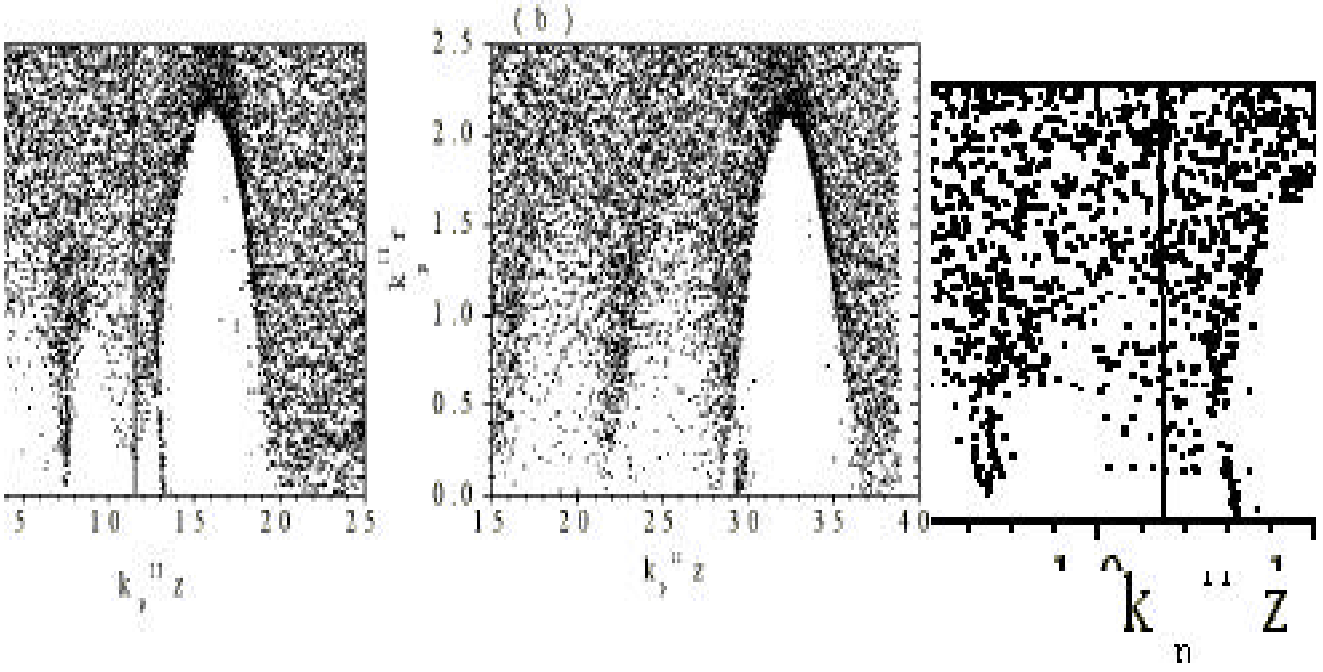

Figure 1

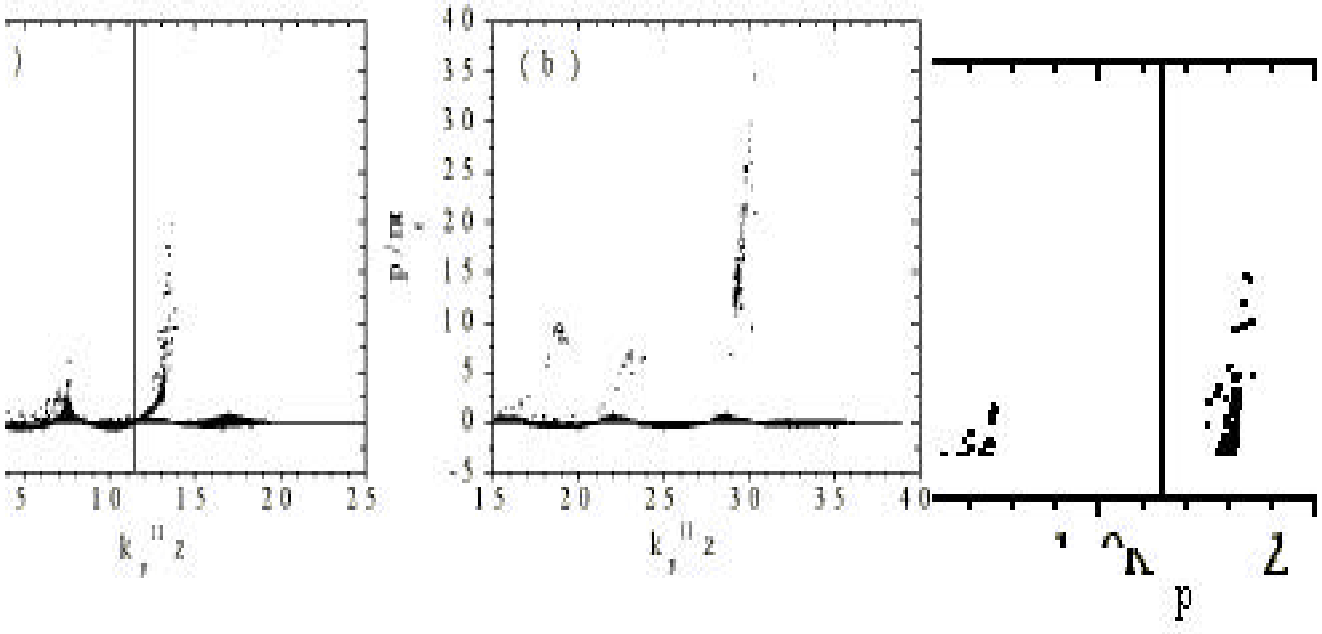
)
(b)
40
35
30
25
20
15
10
5
0
-5
5
10
15
20
25
15
20
25
30
35
40
$k_p^{II}z$
$k_p^{II}z$
p

Figure 2

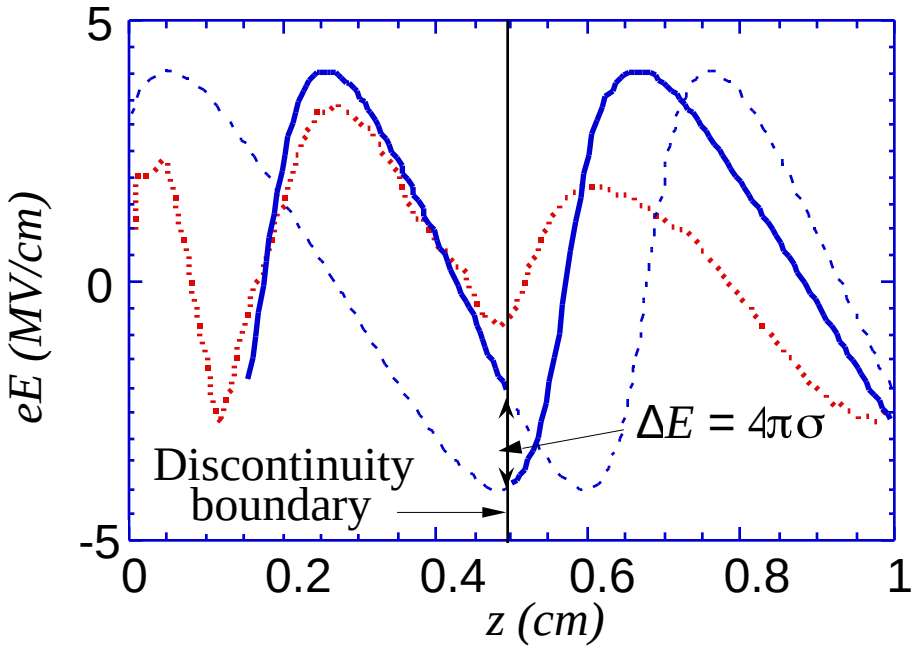

Figure 3

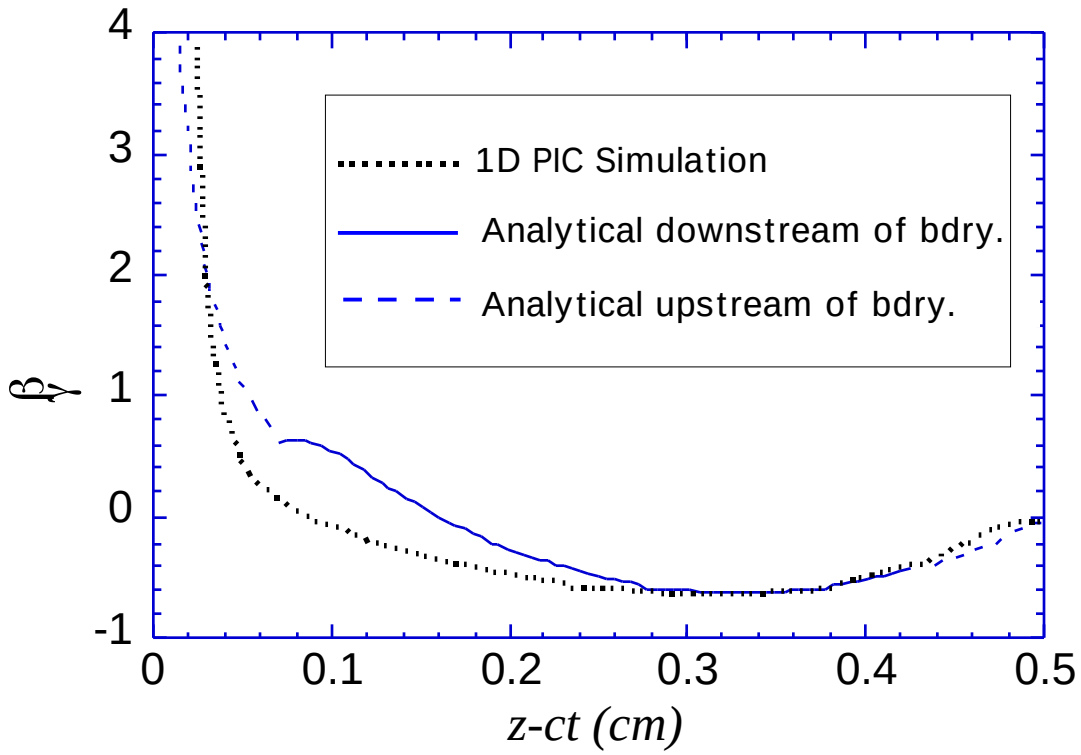
4
3
2
1
0
-1
0
0.1
0.2
0.3
0.4
0.5
βγ
z-ct (cm)
1D PIC Simulation
Analytical downstream of bdry.
Analytical upstream of bdry.

Figure 4